FCCC: Forest Cover Change Calculator User Interface for Identifying Fire Incidents in Forest Region using Satellite Data

Anubhava Srivastava[1], Sandhya Umrao[2], Susham Biswas*[3], Rakesh dubey[4], Md. Iltaf Zafar[5]
Dept. of Computer Science and Engineering
Rajiv Gandhi Institute of Petroleum Technology, Jais, Amethi, Uttar Pradesh, India[1,3,4,5]
Dept. of Computer Science and Engineering
Noida Institute of Engineering & Technology, Uttar Pradesh, India[2]

***Abstract*—For the ecosystem to maintain a balance between the social and environmental spheres, forests play a crucial role. The greatest threat to forests for this significance, is fires and natural disasters caused by several factors. It is crucial to assess the genesis and behavioral characteristics of fires in forest areas. The discovery of the forest fire areas and the intensity of the fire affected are greatly facilitated by the satellite image obtained by different sensors and data sets. We are suggesting a novel approach to compute changes using spectral indices, using landsat-9 and sentinel-2 satellite datasets for measuring the change in forest areas affected by fire accidents over Kochi areas on March 2023. Kochi is a city in Kerala, South India, and is located at 9° 50' 20.7348" N and 77° 10' 13.8828" E. coordinates. Computation is performed by calculating forest area before the fire incident (pre-fire) and after the fire incident (post-fire) and total loss is calculated by the difference between pre-fire and post-fire incident. The proposed work uses Sentinel-2 and Landsat-9 satellite images to recover burn scars using several vegetation indicators. We have identified the fire locations using the object-based classification approach. For verification of results computed by vegetation indices, we have also performed land use land cover classification and calculated the changes in forest areas. Accuracy is computed by the confusion matrix with an accuracy of 89.45% and the kappa coefficient with an accuracy of 87.68%. In particular, there was a strong correlation between forest loss and the burned area in the subtropical evergreen broadleaf forest zone (6.9%) and the deciduous coniferous forest zone (18.9% of the lands). These findings serve as a foundation for future forecasts of fire-induced forest loss in regions with similar climatic and environmental conditions.**

***Keywords*—GEE; remote sensing; classification; landsat; sentinel; forest fire**

I. Introduction

The forest is a foundation for all living things and is crucial in influencing global climate change. The forest is divided into basically three types: Reserved Forest (RF), Protected Forest (PF), and Unclassified Forest (UF). Under federal or state forest legislation, a place is known as a Reserved Forest (RF), which is completely protected. Unless otherwise permitted, no activity is allowed in the reserved forest. The State Forest Act or the Federal Forest Act may designate a territory as a Protected Forest (PF). An unclassified Forest (UF) is a place that has been given a forest designation but is not a restricted or protected forest. Depending on the state, these woodlands may be owned differently. Being the primary categories of natural landscapes, forests are the most priceless natural resources on earth. Unlike other natural resources like minerals, mineral oils, and natural gas, which are finite and cannot be replenished, forests have the amazing advantage of being renewable. However, the productivity of forests depends heavily on human activity. More than four billion acres of forest cover the entire earth, according to a survey by the Global Forest Resource Assessment (GFRA) in 2020 [1] the size of these forests cover varies, and it covers the entire surface of the earth. With around 45% of the world's total forest cover, Europe has the largest forest cover, according to another report from 2011. Considering percentages, South America is the top continent in terms of the area that is covered by forests, with almost half of its land mass falling under forests. If we consider per capita forest area, Oceania is placed first. But a percentage of these forest areas are degraded year to year due to several natural factors or man-made activity. According to the Forest Survey of India in the Year 2023 between the dates 1 March 2023 to 15 March 2023, a total of 772 large fire accidents happened. Mizoram has been affected by a maximum total of 110 fire incidents, and Meghalaya, Manipur, and Assam forest areas have been affected a total of 59, 52, and 43 fire incidents respectively. The reasons behind these fire incidents in forest areas are less precipitation level in February 2023. The country recorded only a 7.2 mm rain level in February which is the sixth lowest from the year 1901, central India recorded 77% rain deficiency while the northwest, southern, and northeast area recorded 76%, 54%, and 43% rain deficiency respectively. Total 38 forest fire incidents were reported in Kerala between January and April of 2018. Kerala had numerous fire events, from January to March 2017; 2,100 hectares were destroyed in 440 fire incidents. The reason behind this incident is climate change; also because one of the factors that contribute to fires is the increase of dryness in the environment. Forest Fires can be identified and characterized by several indicators. The spectral reflectance characteristics of healthy vegetation and burnt scar vegetation can be used to identify forest fires. For fire detection, thermal variations between burning and background pixels are also frequently used. The thermal infrared bands on satellite sensors like ASTER, MODIS, and VIIRS also can be used to detect forest fires. Since the majority of these sensors are categorized as having coarser spatial resolutions, it is challenging to monitor

*Corresponding authors

fires on a regional scale. For instance, burn area products from the Moderate Resolution Imaging Spectroradiometer (MODIS) are available globally in 500 m (MCD64A1) since 2001 [2]. There are a number of researchers who performed change detection due to fire incidents over different land cover areas like [3] performed forest fire area computation over Mugla, Turkey using different vegetation indices. The authors in [4] performed their analysis over the Pacific Northwest, USA for finding the effects of climate change on fire regimes. The rest of the paper is structured as follows. Related work is presented in Section II. Section III illustrates the study area, Section IV presents a methodology and materials like data sets, vegetation indices, and classification algorithms used in the computation. The result is discussed in Section V and in the last Section VI presents the concluding remarks.

II. Related Work

Forests fire occurred in recent years in a very large manner. Remote sensing techniques are mainly used for the finding reason and computing loss for these fire incidents, there are a number of platforms available in geographic information systems (GIS) which are used to calculate these changes like QGIS, ArcGIS, and ELWIS using satellite images. But these GIS softwares required large processing of data before computation, [5] have used such geographic information, system-based software and produced a framework for computing change analysis. In this analysis data sampling was put into place in two primary stages: maintaining a binary map for the burned area and unburned areas and mapping the burned areas of various land cover classes. The primary stage focuses on mainly five steps: removal of cloud cover and other noise (prepossessing), spatial and spectral feature extraction for pre-fire and post-fire, analysis of change in forest area in pre-fire and post-fire computation, extraction of features, mapping of burned areas based on the selection of feature from VIIRS hotspots, but extraction of burned area and unburned area takes a very large amount of time and computation so some researchers used Google Earth Engine for computation and pre-analysis. The authors in [6] have performed their analysis using Google Earth Engine (GEE) [7], over two satellites Landsat 8 and Sentinel 2. The researchers performed their computation by partitioning into four-level, performed the supervised burned area over the cartography tool for stratified random sampling, after the selection of data change in the area over a given time period. In [8] researcher performed his study by use of 14 different sets of fire variables that are taken from spectral vegetation indices, environmental variables, climate factors, and other spatial features. The training and testing validation is performed using a classification algorithm later use bootstrap, and optimistic bootstrap approaches to evaluate the models' accuracy and estimate the variance and bias of the estimate. But these researchers are focusing on the sample and collected data set only not on real-time data sets. Later Andrea Tassi and Marco Vizzari [9] proposed point-based (PB) and object-based (OB) classification and categorization techniques, that may be implemented on the spatial cloud platform, Google Earth Engine (GEE). Ramita Manandhar [10] also studied the framework-based technique of classification to enhance the accuracy of the classification algorithm by combining other data, such as different land cover classes, spatial features, spectral indices, and digital elevation models. The study [11] discusses the other category of classification, he performed categories based on the study of light detection and ranging (LIDAR) was used as part of an innovative strategy for mapping the danger of forest fires. The hierarchy process was used to calculate the criteria weights that affect fire risk and was applied to two different data sets over the different locations of Spain. The findings indicate that about 50 % - 65% of the study area is classified as 3-moderate fire risk zones. The researcher will be able to choose the best vegetation management strategies based on the danger of forest fires according to the technique given in the [11] study. The forest fires problem does not occur only in the global region but also causes in many places in small areas like the valley of the Himalayas. Over the course of the whole research region, the forest fire burn area dramatically fluctuates with time and space. Research [12] concluded that fire problems arose in the west-to-south Himalayan region multiple times between years 2000 -2010. Higher burn area fraction patches (0.7sq-km to 1 sq-km) were discovered over the southeast regions of the eastern Himalayas, the central Himalayas, and the western Himalayas. Over the past two decades (2001–2020), the average yearly burn area was 5557.35 sq-km, with a large amount of variability (standard deviation 2661.71 sq-km). The yearly burn area increased significantly by 755.7 sq-km per year between 2001 and 2010 but declined in the following decade. Further [13] provides three models for anticipated forest fire susceptibility maps (FFSM) using the Google earth engine (GEE) platform and then maps it over geographic information system software. The researcher [14] uses a range of probability mechanisms for finding change due to fire incidents; value lie between 1 to 0 if it surrounds near 1 then occurrence and loss is high and in other case occurrence and loss is very less. Deforestation is the long-term loss of trees as a result of anthropogenic or natural activity. It happens everywhere as a result of intricate socioeconomic processes like population and housing increase, agricultural expansion, and wood exploitation in underdeveloped nations. Deforestation is also made worse by economic, political, technological, and cultural causes. Deforestation contributes to a number of serious issues, such as soil erosion, disruptions to the water cycle, and possibly global repercussions. Deforestation has caused the land to change too quickly, resulting in the loss of vegetation, and wildlife, which hinders the functioning of ecosystems [15], [16] computed the growth in urbanization and loss of forests between the years 2009 and 2019, and found the current trend of urban growth is continuing at a pace of 0.16% each year. Environmentalists and land planners comprehend the effects of land use and land cover to provide recommendations for effective policy strategies to manage growth in Cameron Highlands. The study [17] discussed the forest management systems in Finland and Scandinavia. Satellite images are used in Finland and Sweden's national forest inventories. Researchers [18] witnessed fast changes in land use and cover, with the area covered by vegetation dropping from roughly 46% in 2009 to 28% in 2019. Area of about 27.54 percent of the area covered by vegetation is converted to urban/built-up areas, 4.60 percent to agriculture, and 6 percent to arid terrain. The amount of agriculture and urban/built-up area has greatly expanded. The research [19] analyzed the change in different classes of land cover using a number of sample points and training and testing points for each class. Points are split into subgroups for training

(70%) and evaluation (30%). Metrics obtained from an error matrix were used to measure accuracy. The research [20] describes that global service on SUHI monitoring is available to provide helpful cues for our cities' increasingly sustainable urban design. In [21] the author discusses different spatial resolution and wavelength of satellite Sentinel-2 and Landsat-8 and describe that both satellites are useful and provide good accuracy in measuring changes that occur in a fire-prone area. Sentinel-2 satellites have a spatial resolution of 10 meters while landsat data sets have a spatial resolution of 30 meters. The researcher in [22] states that planning for conservation and management, as well as ecological study, is made more difficult in tropical rainforests due to a dearth of spatially and thematically precise vegetation maps. Such maps have a great deal of potential to be produced by remote sensing, but the categorization accuracy within primary rain forests has typically fallen short of practical uses.

III. Study Area

The study area Fig. 1 is located at 9.50°N and 77.10°E. covering about 2407 square kilometers (1,171sq mi) and bordered on the north by the district of Thrissur, on the south by the districts Kottayam and Alappuzha, on the east by the district Idukki, and on the west by the Arabian Sea. Three separate sections make up the district: Hills and woods, plains, and the seashore, respectively, make up the highland, midland, and lowland regions. The highlands are located at a height of around 300 m. (980 ft). Except for Muvattupuzha, the Periyar River, Kerala's longest, traverses every taluk. The district is traversed by the Chalakkudy River and the Muvattupuzha River.

It consists of several land cover classes like urban, water, and forest (high vegetation), agriculture (low vegetation) but forest alone consists of 45.20% of total land. In the year 2022-23, a total of nearly 430.75 hectares was affected by 391 fire incidents. According to data from the state pollution control board, the mean air quality index remained above 300 $PM_{2.5}$ (particulate matter) concentrations in the air for five days before the fire occurrence.

It was 441 $PM_{2.5}$ concentrations on March 5; 445 $PM_{2.5}$ concentrations on March 6; 465 $PM_{2.5}$ concentrations on March 7; 324 $PM_{2.5}$ concentrations on March 8; and 380 $PM_{2.5}$ concentrations on March 9. Good breathable air quality has an index value of less than 50 $PM_{2.5}$ concentrations, while before the dump yard fire, the city's average air quality index was below 100 $PM_{2.5}$ concentrations. The study area is computed as 3,432 mm of rain falls on average in the district this year. The district has a mild temperature average temperature between May 2022 to March 2023 as shown in Fig. 2.

The temperature rapidly increases during fire time and is largely located in the Malabar Coast moist forests ecoregion, while the highlands are a part of the South-Western Ghats moist deciduous forests ecoregion. On the border of the districts of Ernakulam and Idukki, the Anamudi is the tallest mountain in South India. Sholas can be found in some areas of the Mankulam Forest Division and Idamalayar Reserve Forest, however, these areas cannot be reached by road. Edamalakkudy and the Idamalayar Protected Forest, have different kinds of rocks, silt, and sand. The majority of the district's eastern forests are secluded and are a portion of the Anamalais. Temperature is also a very significant factor after the forest fire incident it changed moderately.

IV. Materials and Methods

Since the 1970s, surface soil moisture (SSM) and change in the surface area has been determined by remote sensing. The primary benefit of remote sensing is that it offers geographically diverse data, as surface variables with spatial information are necessary for many applications, including evapotranspiration evaluation, soil erosion mitigation, irrigation scheduling, drought monitoring, and forest management.

The study is performed by using the satellite data set from Sentinel and Landsat over the cloud platform Google Earth Engine (GEE). GEE is a planetary platform that has access to different satellite data like Sentinel, Landsat, MODIS, etc. Each satellite has the unique characteristic as wavelength, band combination, and resolution. Here we are accessing sentinel-2 and Landsat-9 to observe forest area changes. A detailed description of the analysis is shown in the Fig. 3 and used bands used for analysis by both data sets are detailed in Table I.

Research is subdivided into two parts. We calculate the change in forest area from pre-fire and post-fire accidents. Later we perform observation over the burn area and calculate the different changes in the forest area. These changes are calculated by computing the change in a land cover class by the gradient tree boost classification model and also by computing the change in mean and standard deviation value of different indices like Green Normalized Difference Vegetation, Adjusted Transformed Soil Adjusted Vegetation Index (ATSAVI), Normalize difference water index (NDWI) and Enhance vegetation index (EVI). The methodology used in the research is illustrated in Fig. 3. GNDVI (Green Normalized Difference Vegetation) measures the "greenness" or photosynthetic activity of plants. While it saturates later than NDVI, it is a chlorophyll index that is utilized during later phases of development. It is one of the most popular vegetation indices for calculating crop canopy water and nitrogen uptake. The values for Normalize difference water index (NDWI), like other indices, range from -1 to 1, with high values denoting high plant water content and coverage of a significant portion of the plant and low values denoting low vegetation water content and sparse cover. Pre-fire and post-fire results are calculated by using the normalized burn ratio mechanism and calculated by equation 1.

$$NBR = \frac{(NIR - SWIR)}{(NIR + SWIR)} \tag{1}$$

Where: NIR (Near Infra-Red) as a Band 5
SWIR (Short Wave Infra-Red) as a Band 7

GNDVI has a greater saturation point than NDVI and is more sensitive to changes in the crop's chlorophyll content. While NDVI is useful for predicting crop vigor in the early stages, it can be used in crops with dense canopies or in more mature phases of growth.

$$GNDVI = \frac{NIR - GREEN}{NIR + GREEN} \tag{2}$$

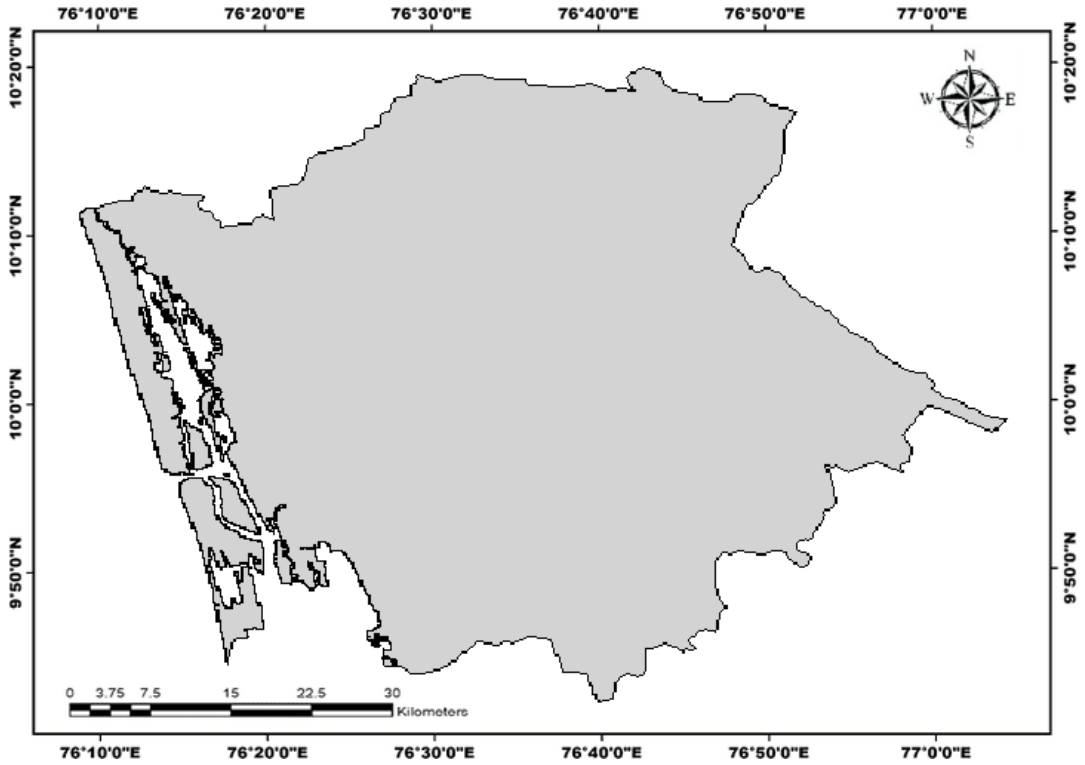

Fig. 1. Study area.

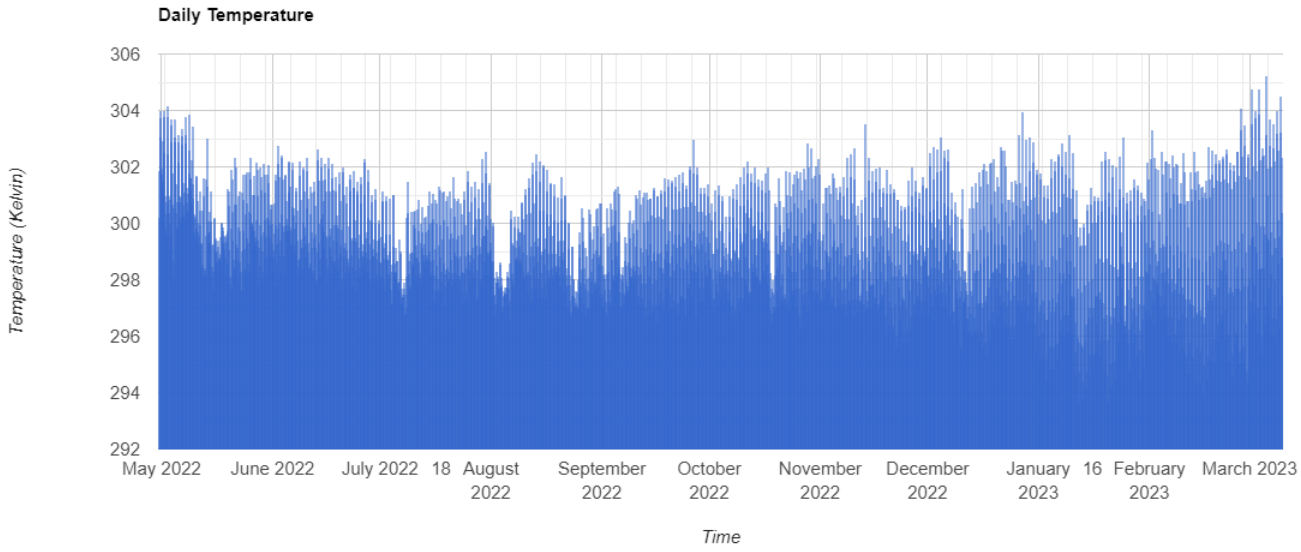

Fig. 2. Daily average temperature in study area between May 2022 and March 2023.

Where: NIR: Near Infra-Red
GREEN: GREEN Wavelength Band
A water body can "stand out" against the land and vegetation by using the Normalized Difference Water Index (NDWI) to emphasize open water features in a satellite picture.

$$NDWI = \frac{GREEN - NIR}{GREEN + NIR} \quad (3)$$

Where: NIR: Near Infra-Red
GREEN: GREEN Wavelength Band
The normal reflectivity of the sea surface is maximized in

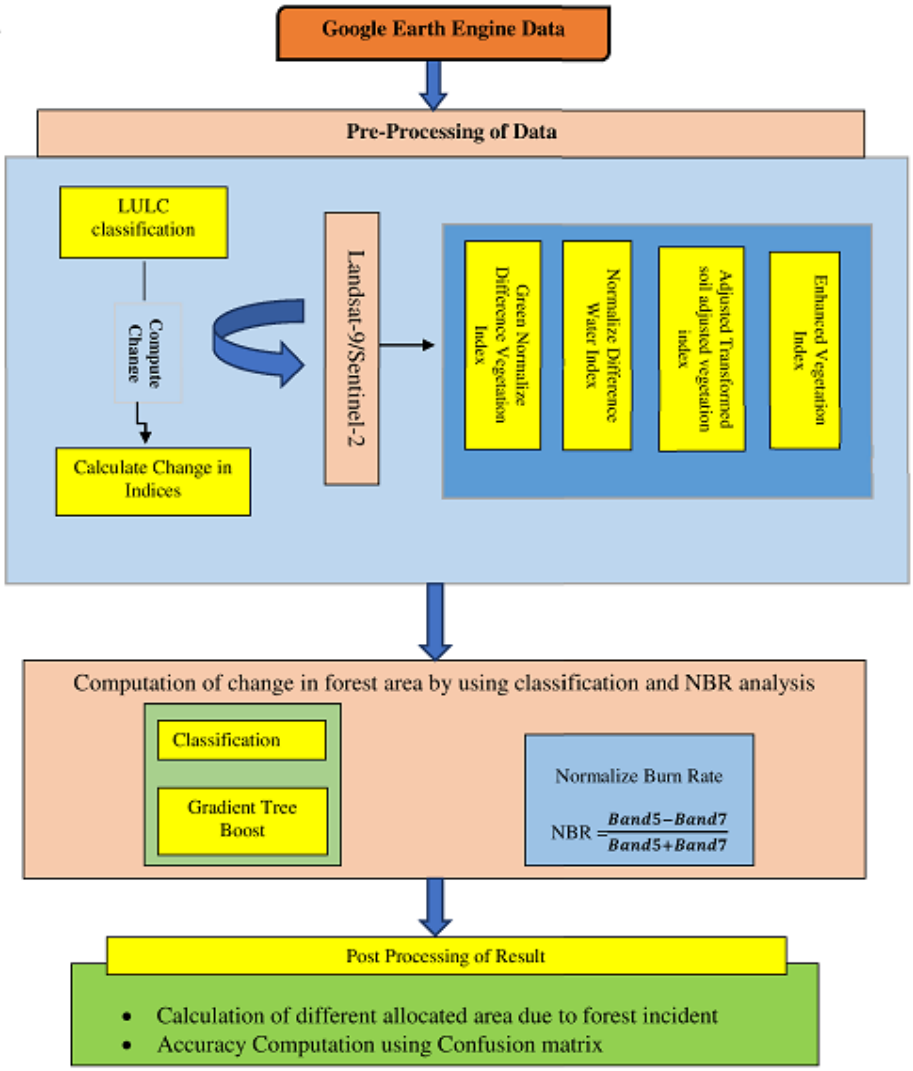

Fig. 3. Methodology used in the research.

the visible green wavelengths. The near-infrared wavelengths maximize the high reflectance of terrestrial vegetation and soil components while minimizing the low reflection of aquatic features. The NDWI equation yields positive values for water features and negative ones (or zero) for soil and terrestrial vegetation.

$$EVI = \frac{2.5 * (Band5 - Band4)}{(Band5 + 6 * Band4 - 7.5 * Band2 + 1)} \quad (4)$$

In dense vegetation, EVI is more sensitive and can compensate for some atmospheric conditions and canopy background noise. While ATSAVI is used where vegetation cover is very low.

$$ATSAVI = a\frac{(NIR - a * RED - b)}{((a * NIR) + (RED - a * b) + (X * (1 + a^2))} \quad (5)$$

Classification is performed using the Gradient tree boost machine learning classifier algorithm [23]. It provides a hypothetical model in the form of an ensemble of decision trees. Mainly it is a collection of nodes of weak prediction models. The resulting technique, called gradient-boosted trees, typically it beats random forest when a decision tree is a weak learner. The construction of a gradient-boost trees model follows the same stage-wise process as previous boosting techniques, but it generalizes other techniques by optimizing any differentiable loss function, later we computed accuracy by using the confusion matrix by equation 6 and kappa coefficient by equation 7. Cohen recommended the following interpretation of the Kappa result: values 0 as showing no agreement and 0.01-0.20 as none to the partial agreement, 0.21-0.40 as fair agreement, 0.41- 0.60 as moderate agreement, 0.61-0.80 as significant agreement, and 0.81-1.00 as almost perfect agreement.

$$Accuracy = \frac{TP + TN}{TP + TN + FP + FN} \quad (6)$$

Where TP= True Positive,
FP = False Positive

TABLE I. BAND USES FOR CALCULATING CHANGES IN FOREST COVER

COLOR	LANDSAT		SENTINEL	
	BAND	WAVE LENGTH	BAND	WAVE LENGTH
BLUE	BAND - 2	0.45 - 0.51	BAND - 2	0.492 - 0.496
GREEN	BAND - 3	0.53 - 0.59	BAND - 3	0.559 - 0.560
RED	BAND - 4	0.63 - 0.67	BAND - 4	0.664 - 0.665
NIR	BAND - 5	0.85 - 0.87	BAND - 8	0.833 - 0.835
SWIR	BAND - 7	2.1 - 2.2	BAND - 12	2.18 - 2.20

$\bar{T}N$ = True Negative,
$\bar{F}N$ = False Negative

$$\kappa\& = \frac{P_o - P_e}{1 - P_e}. \quad (7)$$

Where P_o = Observed proportional agreement,

P_e = Hypothetical probability of chance agreement.

V. RESULT

Deforestation is taking place day to day in a very large manner, sometimes it is being done by human activity, and sometimes it is by natural activity, like flood, and fire. We are calculating a change in the forest area of Kochi district from all the above mention activity. The primary reason for the change in forest area over the study area is some fire accidents that occurred between January 2023 and March 2023. But we are not only rigid for these fire issues we also calculate all other possible reasons also for deforestation. So here we calculated vegetation indices like NDVI (Normalize Difference Vegetation Index), GNDVI (Green Normalize Difference Vegetation Index), ATSAVI (Adjusted Transformed Soil Vegetation Index), and EVI (Enhanced Vegetation Index). These vegetation indices are used for the calculation of Change of Vegetation indices and also for evaluating the effect on soil moisture and water due to these changes. For the calculation of forest change in the study area we first calculate the change as shown in Fig. 4 and Fig. 5 using a supervised classification technique Gradient Tree Boosting. For this, we calculated about 1200 data points of different land cover classes and took 70% data as training points and 30% data as testing points. Results of this classification are shown in Fig. 4 and Fig. 5 and these changes are described that a large amount of forest loss occurred by these fire incidents. So for calculating these losses here, we computed the percentage of the forest before the fire incident (pre-fire) and after the fire incident (post-fire). After classification, we computed the accuracy of the classification result by confusion matrix and kappa coefficient, total accuracy computed by confusion matrix is 89.45% and by kappa coefficient is 87.68%. On focusing output generated by the gradient tree boost in Fig. 4 and Fig. 5, there is a lot of change happening in the east-south region of the study area. The reason behind these changes is fire accidents in these areas. So we calculate fire accidents in this area, mainly two major fire accidents found at two places, and many vegetation changes occur due to this fire accident. Fig. 6 and Fig. 7 shows the change in vegetation due to these fire accidents in the study area.

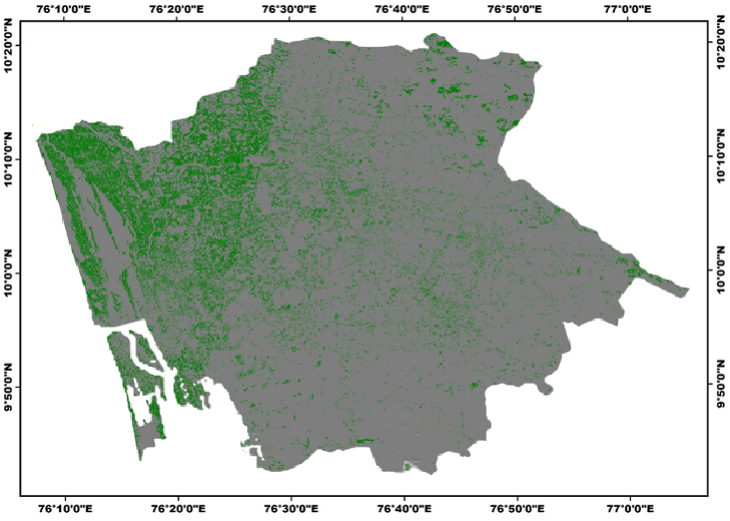

Fig. 4. Output generated over landsat-9 data sets before fire incident.

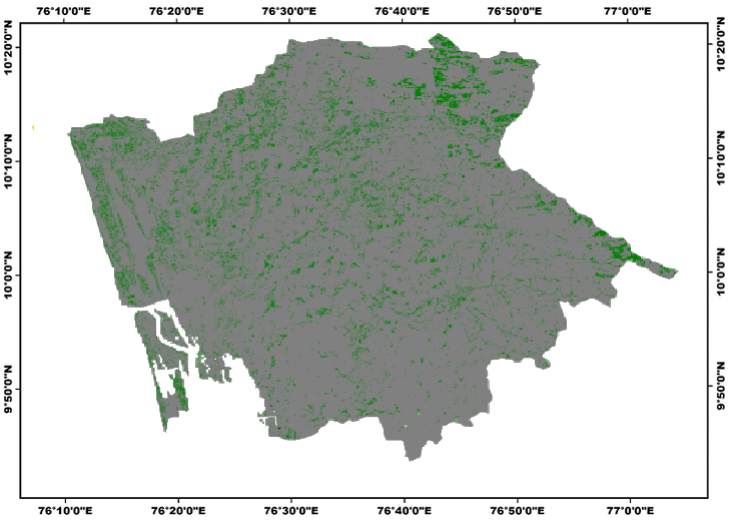

Fig. 5. Output generated over landsat-9 data sets after fire incident.

Fig. 8 shows the loss of land cover areas during a fire incident. The fire affected approximately 24.67% of land cover

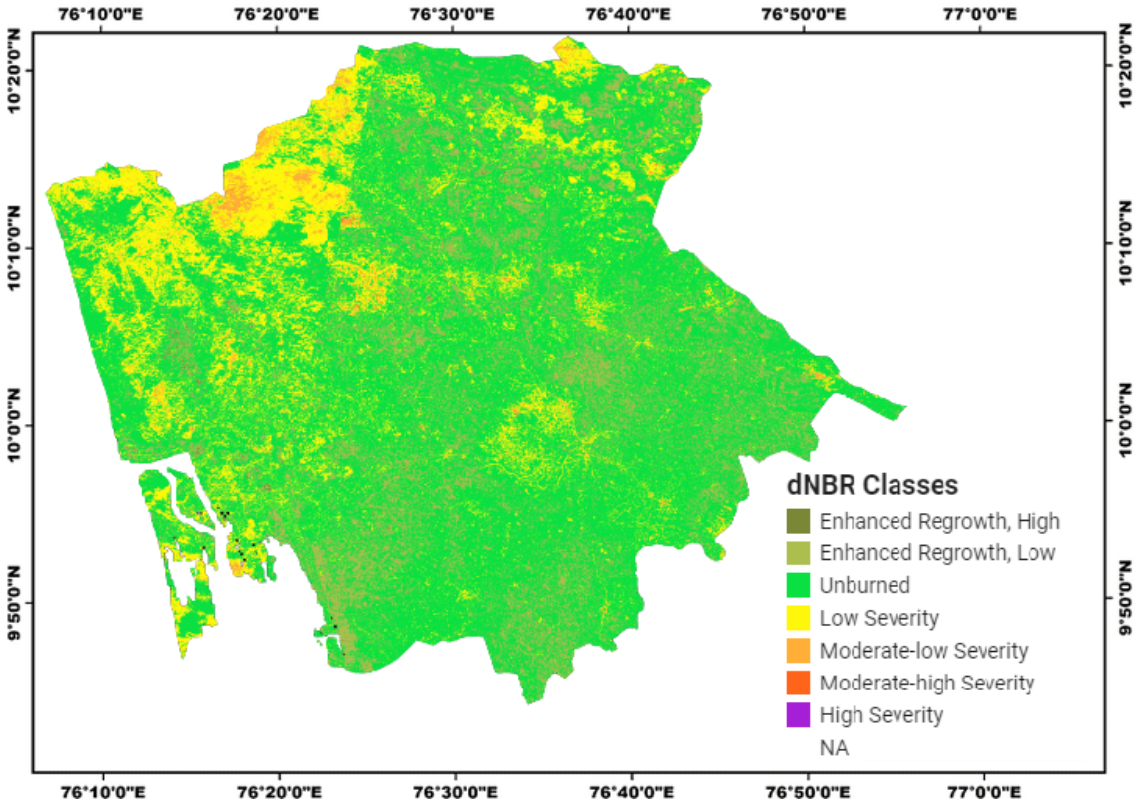

Fig. 6. Fire incidents happened between January and February months.

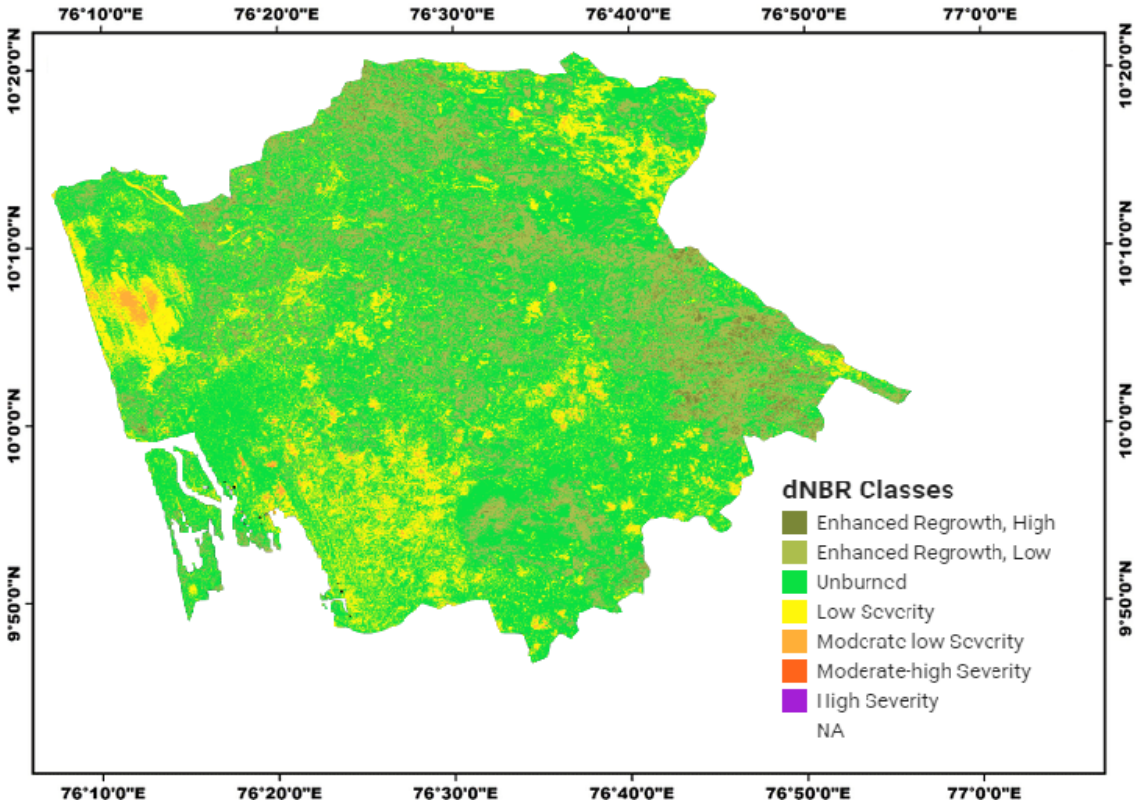

Fig. 7. Fire incidents happened between February and March months.

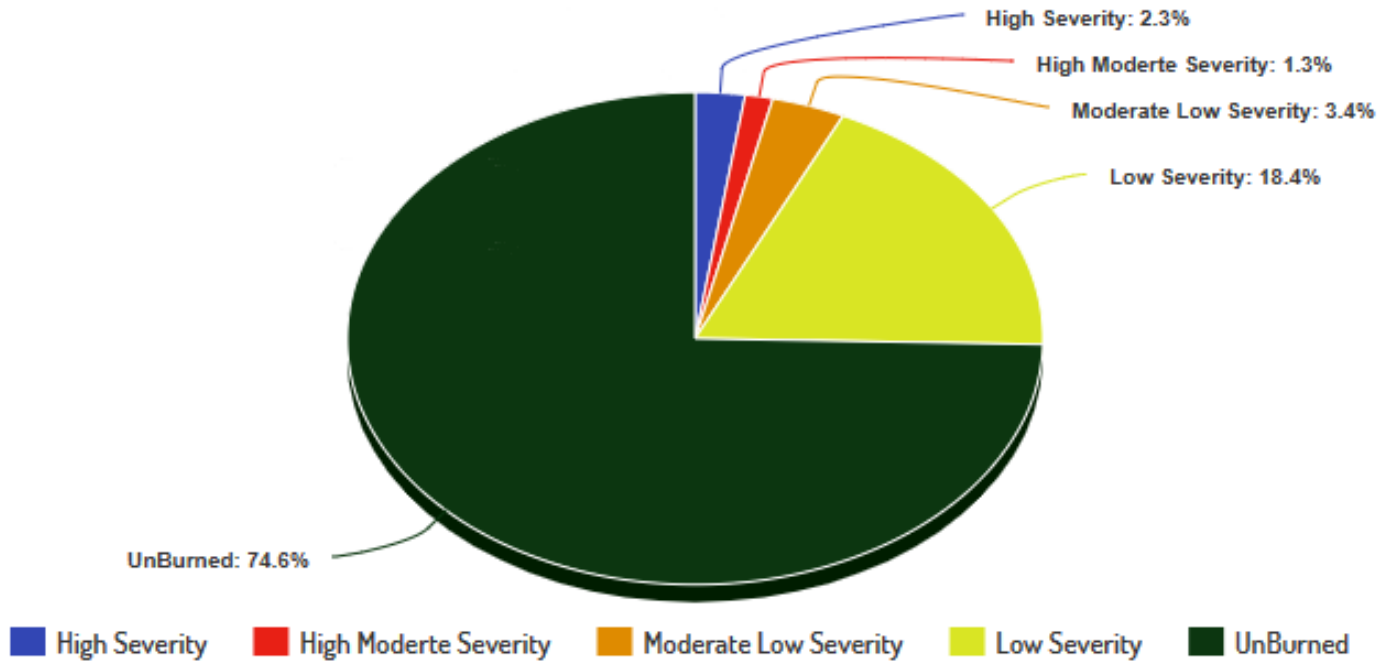

Fig. 8. Changes in the study area.

areas. These areas come under dense forest, moderate dense forest, open forest, and scrubland as we computed here forest loss. So non-forest areas about 74% are detected as having no loss.

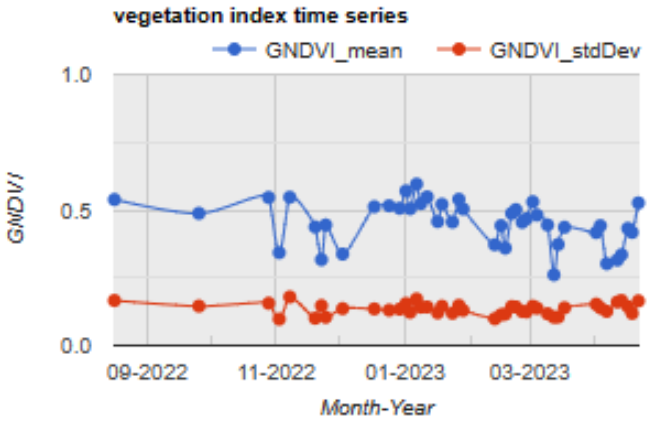

Fig. 9. Green normalize difference vegetation index calculated over study area during forest fire using sentinel 2 data set.

Green Normalize Difference Vegetation index, Normalize Difference Water Index, Adjusted Transformed Soil Adjusted Vegetation Index. Enhanced Vegetation Index is calculated over Ernakulum during the forest fire time from September 2022 to March 2023. We found that time when rapid fire arises, its mean and standard deviation value change. For verification purposes, we have computed the mean GNDVI over two data sets Landsat-9 and Sentinel-2.

These two data sets are easily available in the Google Earth Engine directory; basic difference between both data sets in

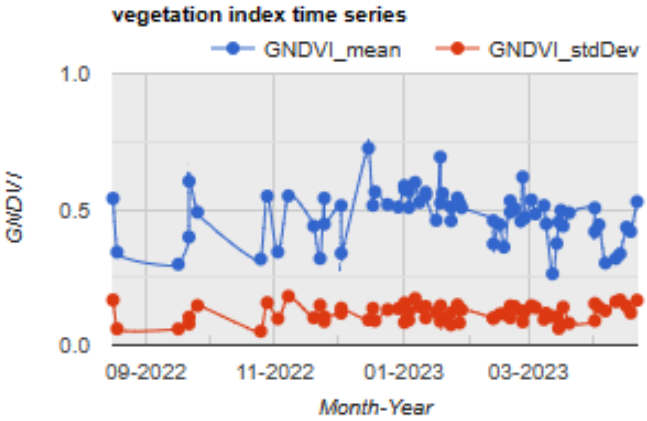

Fig. 10. Green normalize difference vegetation index calculated over study area during forest fire using landsat 9 data set.

terms of resolution is Landsat-9 data sets having a resolution of 30 meters and Sentinel data sets having a resolution of 10 meters, these data sets also have a collection of nine different bands each band having unique attributes and the ratio of these bands providing a different signature for each vegetation indices. Fig. 9 and Fig. 10 show the change in green normalize difference vegetation index over sentinel-2 and landsat -9 data sets respectively and both data sets have nearly the same result over the study area. Later we calculate mean and standard deviation values over normalized difference water index (NDWI), adjusted transformed soil adjusted vegetation index (ATSAVI), and enhanced vegetation index (EVI). For observing the effects of fire incidents over water, soil, and natural vegetation indices. Fig. 11, and Fig. 12 shows results

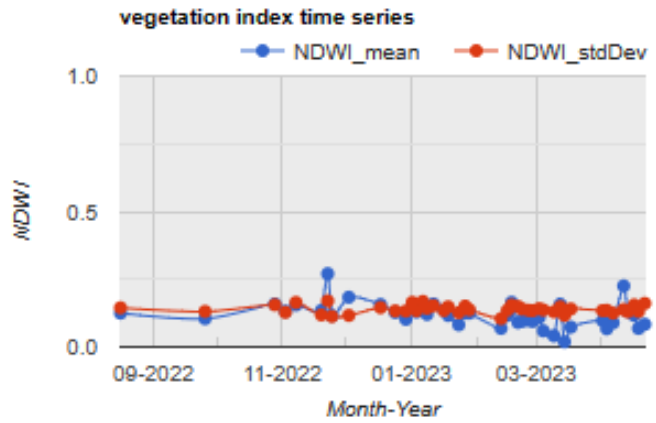

Fig. 11. Normalize difference water index calculated over study area during forest fire using sentinel 2 data set.

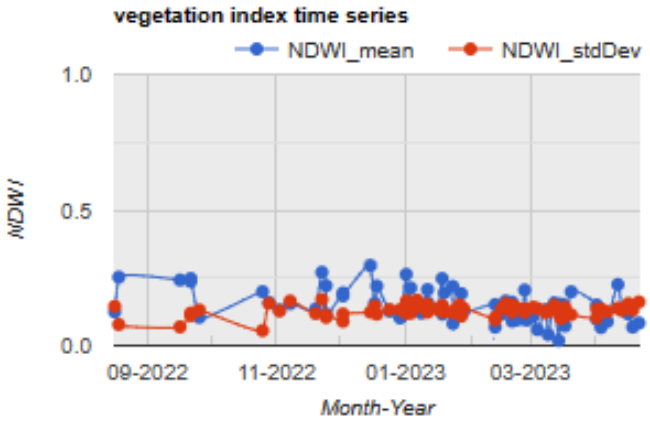

Fig. 12. Normalize difference water index calculated over study area during forest fire using landsat 9 data set.

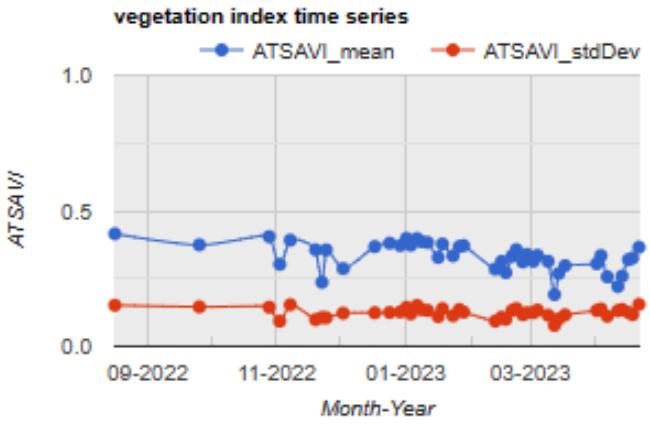

Fig. 13. Adjusted transformed soil adjusted vegetation index calculated over study area during forest fire using sentinel 2 data set.

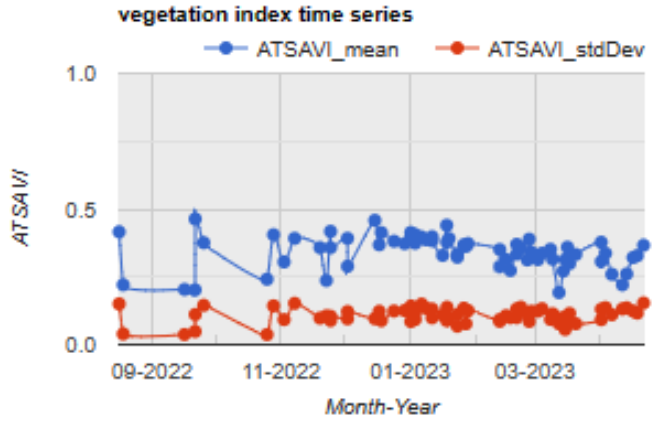

Fig. 14. Adjusted Transformed Soil Adjusted Vegetation index calculated over study area during forest fire time using landsat 9 data set.

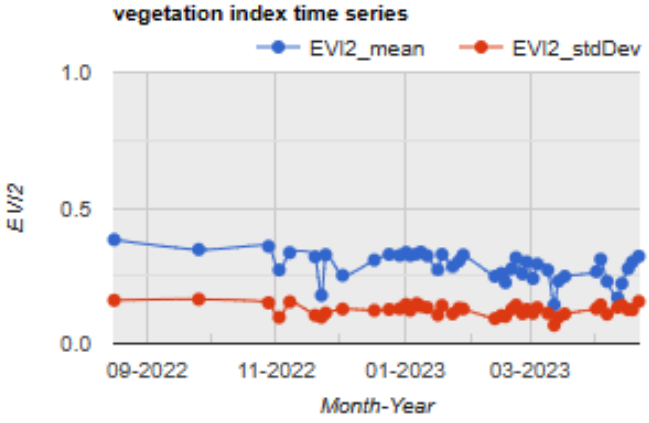

Fig. 15. Enhanced vegetation index calculated over study area during forest fire using sentinel 2 data set.

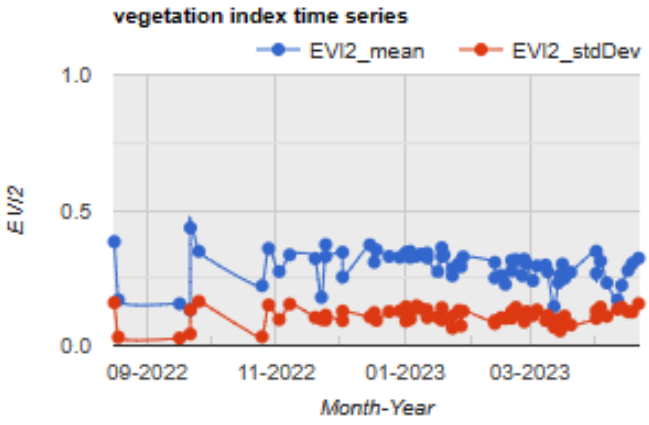

Fig. 16. Enhanced vegetation index calculated over study area during forest fire using landsat 9 data set.

for normalized difference water index, Fig. 13 and Fig. 14 show result for adjusted transformed soil adjusted vegetation index, and Fig. 15 and Fig. 16 shows the result obtained from

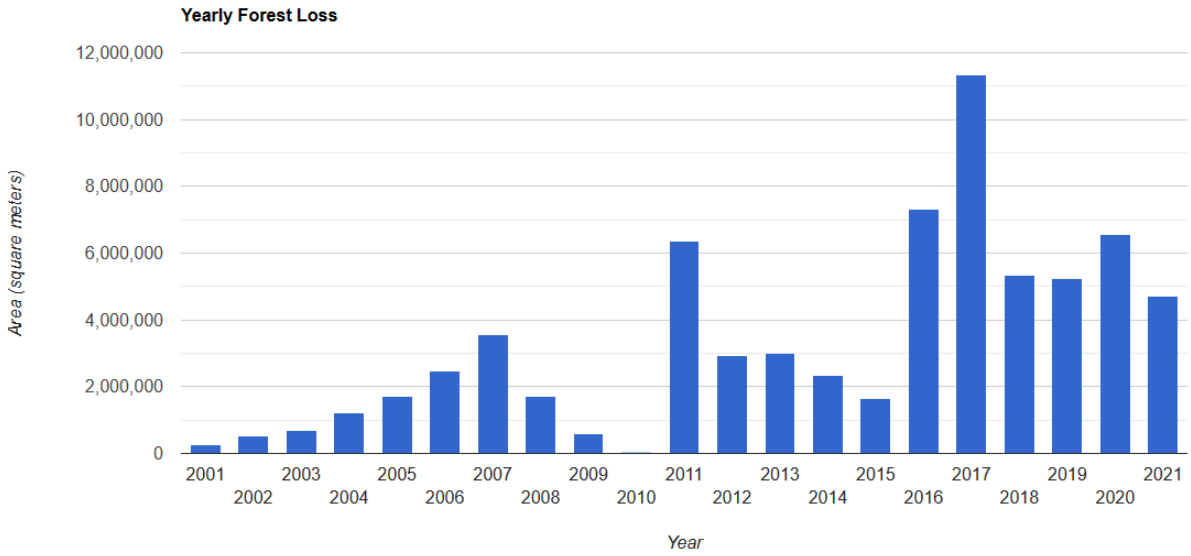

Fig. 17. Forest loss computed from year 2000 to year 2023.

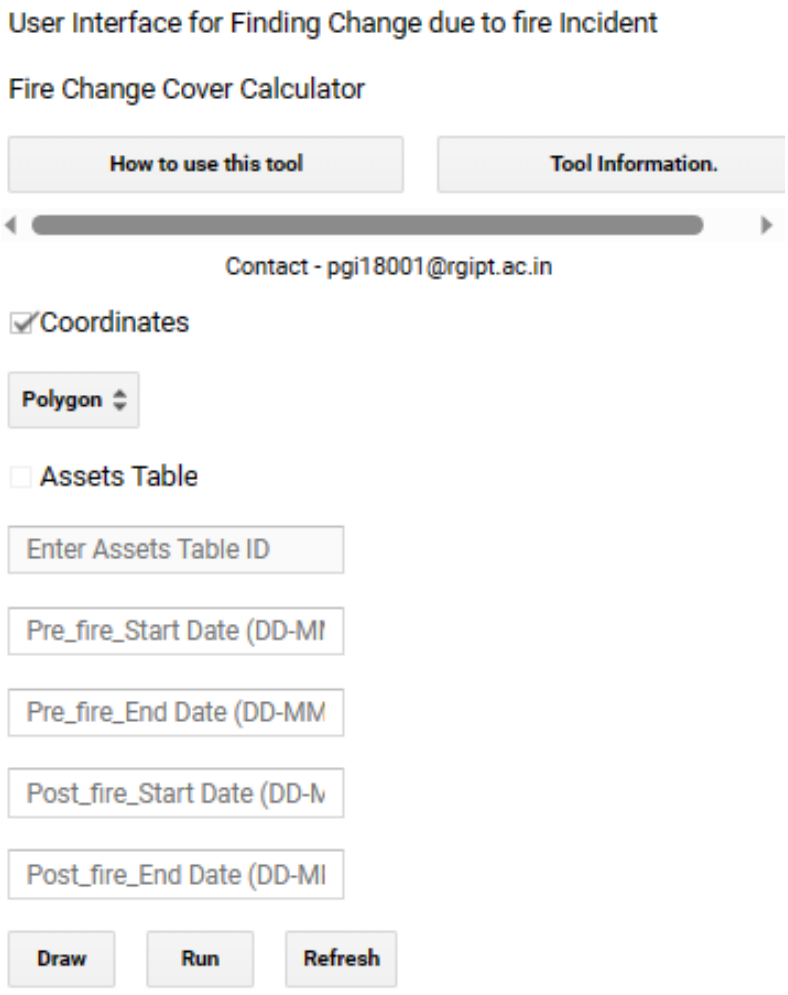

Fig. 18. Snip of user interface available at https://paper1.users.earthengine.app/view/forest-cover-change.

enhanced vegetation index over Sentinel-2 and Landsat -9 data sets respectively; this result shows that change in these indices occurred at the time of fire incident over the study area and also after the fire incident also. From the above observations, we find that fire forest reduces greenery as well as affects water and soil also. Equations (1 to 5) are used for the calculation of these indices and finding change during fire incidents. Equation 1 is used for calculating a change in the study area due to fire incidents and providing details results which are shown in Fig. 6 and Fig. 7. Areas affected by these fire incidents are described in Fig. 8. From the result, it is shown that a large area of forest loss nearly happened over the study area due to fire incidents. These fire incidents not only disrupted climate conditions and global warming but also had a huge effect on soil and other vegetation indices. We have calculated total forest loss from the year 2000 to the year 2021 using Hansen forest loss cover analysis data sets, and find loss increased from the year 2017 due to multiple reasons over the study area. Detailed analysis of loss cover is shown in Fig. 17

Later at the end, we develop an application user interface that collects data in the form of geometry or if the user has their shape or CSV file of the study area can provide a path in user access link. Users can select desired geometry in the form of a point, polygon, or in rectangle form. A snip of the User interface is located in Fig. 18.

VI. Conclusion

The proposed analysis model is used to compute forest loss in Ernakulum (Kochi) using Landsat-9 OLI, and Sentinels 2 satellite data due to the occurrence of the fire incident. Through our analysis, we found deciduous forests are more vulnerable to fires. About 18.2% of vegetation area was affected by fires in 2023. Among all types of vegetation classes, vegetation that has higher density is affected most by the fire incident. Fire not only destroys vegetation cover but also has an impact on soil and water as well as on climate conditions also. We are also focused on finding factors behind these multiple fire occurrences over study and find an increase in temperature always increases the probability of fire occurrence. We have computed our analysis with more than 85% accuracy. Later our objective is to develop a model that can be used for analyzing change due to fire or another natural disaster by a number of vegetation indices using our defined model.

References

[1] C. D. R. Foundation, Main report. 2020. doi: 10.4324/9781315184487-1.

[2] S. T. Piralilou et al., "A Google Earth Engine Approach for Wildfire Susceptibility Prediction Fusion with Remote Sensing Data of Different Spatial Resolutions," Remote Sens., vol. 14, no. 3, pp. 1–26, 2022, doi: 10.3390/rs14030672.

[3] Kurnaz, "Forest Fire Area Detection by Using Landsat-8 and Sentinel-2 Satellite Images: A Case Study in Mugla, Turkey," vol. 1, no. 2004, pp. 2234–2239, 2007.

[4] J. E. Halofsky, D. L. Peterson, and B. J. Harvey, "Changing wildfire, changing forests: the effects of climate change on fire regimes and vegetation in the Pacific Northwest, USA," Fire Ecol., vol. 16, no. 1, 2020, doi: 10.1186/s42408-019-0062-8.

[5] S. T. Seydi, M. Akhoondzadeh, M. Amani, and S. Mahdavi, "Wildfire damage assessment over Australia using sentinel-2 imagery and modis land cover product within the google earth engine cloud platform," Remote Sens., vol. 13, no. 2, pp. 1–30, 2021, doi: 10.3390/rs13020220.

[6] E. Roteta, A. Bastarrika, M. Franquesa, and E. Chuvieco, "Landsat and sentinel-2 based burned area mapping tools in google earth engine," Remote Sens., vol. 13, no. 4, pp. 1–30, 2021, doi: 10.3390/rs13040816.

[7] N. Gorelick, M. Hancher, M. Dixon, S. Ilyushchenko, D. Thau, and R. Moore, "Google Earth Engine: Planetary-scale geospatial analysis for everyone," Remote Sens. Environ., vol. 202, pp. 18–27, 2017, doi: 10.1016/j.rse.2017.06.031.

[8] B. Kalantar, N. Ueda, M. O. Idrees, S. Janizadeh, K. Ahmadi, and F. Shabani, "Forest fire susceptibility prediction based on machine learning models with resampling algorithms on remote sensing data," Remote Sens., vol. 12, no. 22, pp. 1–24, 2020, doi: 10.3390/rs12223682.

[9] A. Tassi and M. Vizzari, "Object-oriented lulc classification in google earth engine combining snic, glcm, and machine learning algorithms," Remote Sens., vol. 12, no. 22, pp. 1–17, 2020, doi: 10.3390/rs12223776.

[10] R. Manandhar, I. O. A. Odehi, and T. Ancevt, "Improving the accuracy of land use and land cover classification of landsat data using post-classification enhancement," Remote Sens., vol. 1, no. 3, pp. 330–344, 2009, doi: 10.3390/rs1030330.

[11] A. Novo, N. Fariñas-álvarez, J. Martínez-Sánchez, H. González-Jorge, J. M. Fernández-Alonso, and H. Lorenzo, "Mapping forest fire risk—a case study in Galicia (Spain)," Remote Sens., vol. 12, no. 22, pp. 1–21, 2020, doi: 10.3390/rs12223705.

[12] S. Bar, B. R. Parida, A. C. Pandey, and N. Kumar, "Pixel-Based Long-Term (2001–2020) Estimations of Forest Fire Emissions over the Himalaya," Remote Sens., vol. 14, no. 21, 2022, doi: 10.3390/rs14215302.

[13] Y. Piao, D. Lee, S. Park, H. G. Kim, and Y. Jin, "Forest fire susceptibility assessment using google earth engine in Gangwon-do, Republic of Korea," Geomatics, Nat. Hazards Risk, vol. 13, no. 1, pp. 432–450, 2022, doi: 10.1080/19475705.2022.2030808.

[14] Anubhava Srivastava, Sandhya Umrao and Susham Biswas, "Exploring Forest Transformation by Analyzing Spatial-temporal Attributes of Vegetation using Vegetation Indices" International Journal of Advanced Computer Science and Applications(IJACSA), 14(5), 2023. http://dx.doi.org/10.14569/IJACSA.2023.01405114

[15] M. A. Brovelli, Y. Sun, and V. Yordanov, "Monitoring forest change in the amazon using multi-temporal remote sensing data and machine learning classification on Google Earth Engine," ISPRS Int. J. Geo-Information, vol. 9, no. 10, 2020, doi: 10.3390/ijgi9100580.

[16] D. H. J. Aik, M. H. Ismail, and F. M. Muharam, "Land use/land cover changes and the relationship with land surface temperature using landsat and modis imageries in Cameron Highlands, Malaysia," Land, vol. 9, no. 10, pp. 1–23, 2020, doi: 10.3390/land9100372.

[17] H. Astola, T. Häme, L. Sirro, M. Molinier, and J. Kilpi, "Comparison of Sentinel-2 and Landsat 8 imagery for forest variable prediction in boreal region," Remote Sens. Environ., vol. 223, no. January, pp. 257–273, 2019, doi: 10.1016/j.rse.2019.01.019.

[18] A. Srivastava and S. Biswas, "Analyzing Land Cover Changes over Landsat-7 Data using Google Earth Engine," Proc. 3rd Int. Conf. Artif. Intell. Smart Energy, ICAIS 2023, no. Icais, pp. 1228–1233, 2023, doi: 10.1109/ICAIS56108.2023.10073795.

[19] A. Srivastava, S. Bharadwaj, R. Dubey, V. B. Sharma, and S. Biswas, "Mapping Vegetation and Measuring the Performance of Machine Learning Algorithm in Lulc Classification in the Large Area Using Sentinel-2 and Landsat-8 Datasets of Dehradun As a Test Case," Int. Arch. Photogramm. Remote Sens. Spat. Inf. Sci. - ISPRS Arch., vol. 43, no. B3-2022, pp. 529–535, 2022, doi: 10.5194/isprs-archives-XLIII-B3-2022-529-2022.

[20] R. Ravanelli et al., "Monitoring the Impact of Land Cover Change on Surface Urban Heat Island through Google Earth Engine: Proposal of a Global Methodology, First Applications and Problems," pp. 1–21, doi: 10.3390/rs10091488.

[21] G. Forkuor, K. Dimobe, I. Serme, and J. E. Tondoh, "Landsat-8 vs. Sentinel-2: examining the added value of sentinel-2's red-edge bands to land-use and land-cover mapping in Burkina Faso," GIScience Remote Sens., vol. 55, no. 3, pp. 331–354, 2018, doi: 10.1080/15481603.2017.1370169.

[22] K. J. Salovaara, S. Thessler, R. N. Malik, and H. Tuomisto, "Classification of Amazonian primary rain forest vegetation using Landsat ETM + satellite imagery," vol. 97, pp. 39–51, 2005, doi: 10.1016/j.rse.2005.04.013.

[23] J. H. Friedman, "Greedy function approximation: A gradient boosting machine," Ann. Stat., vol. 29, no. 5, pp. 1189–1232, 2001, doi: 10.1214/aos/1013203451.